

## ORIGINAL ARTICLE

# Linking N<sub>2</sub>O emissions from biochar-amended soil to the structure and function of the N-cycling microbial community

Johannes Harter<sup>1,4</sup>, Hans-Martin Krause<sup>1,4</sup>, Stefanie Schuettler<sup>1</sup>, Reiner Ruser<sup>2</sup>, Markus Fromme<sup>3</sup>, Thomas Scholten<sup>3</sup>, Andreas Kappler<sup>1</sup> and Sebastian Behrens<sup>1</sup>

<sup>1</sup>Geomicrobiology and Microbial Ecology, Center for Applied Geosciences, University of Tuebingen, Tuebingen, Germany; <sup>2</sup>Fertilisation and Soil Matter Dynamics, Institute of Crop Science, University of Hohenheim, Stuttgart, Germany and <sup>3</sup>Soil Science and Geomorphology, Department of Geography, University of Tuebingen, Tuebingen, Germany

**Nitrous oxide (N<sub>2</sub>O) contributes 8% to global greenhouse gas emissions. Agricultural sources represent about 60% of anthropogenic N<sub>2</sub>O emissions. Most agricultural N<sub>2</sub>O emissions are due to increased fertilizer application. A considerable fraction of nitrogen fertilizers are converted to N<sub>2</sub>O by microbiological processes (that is, nitrification and denitrification). Soil amended with biochar (charcoal created by pyrolysis of biomass) has been demonstrated to increase crop yield, improve soil quality and affect greenhouse gas emissions, for example, reduce N<sub>2</sub>O emissions. Despite several studies on variations in the general microbial community structure due to soil biochar amendment, hitherto the specific role of the nitrogen cycling microbial community in mitigating soil N<sub>2</sub>O emissions has not been subject of systematic investigation. We performed a microcosm study with a water-saturated soil amended with different amounts (0%, 2% and 10% (w/w)) of high-temperature biochar. By quantifying the abundance and activity of functional marker genes of microbial nitrogen fixation (*nifH*), nitrification (*amoA*) and denitrification (*nirK*, *nirS* and *nosZ*) using quantitative PCR we found that biochar addition enhanced microbial nitrous oxide reduction and increased the abundance of microorganisms capable of N<sub>2</sub>-fixation. Soil biochar amendment increased the relative gene and transcript copy numbers of the *nosZ*-encoded bacterial N<sub>2</sub>O reductase, suggesting a mechanistic link to the observed reduction in N<sub>2</sub>O emissions. Our findings contribute to a better understanding of the impact of biochar on the nitrogen cycling microbial community and the consequences of soil biochar amendment for microbial nitrogen transformation processes and N<sub>2</sub>O emissions from soil.**

*The ISME Journal* (2014) 8, 660–674; doi:10.1038/ismej.2013.160; published online 26 September 2013

**Subject Category:** Geomicrobiology and microbial contributions to geochemical cycles

**Keywords:** nitrogen cycle; biochar; denitrification; nitrification; nitrous oxide; *nosZ*; N<sub>2</sub>O emission; greenhouse gas; soil microbial community

## Introduction

Mankind's increased combustion of fossil fuels and demand for nitrogen in agriculture and industry continuous to impact the global biogeochemical cycling of nitrogen (Galloway *et al.*, 2008). The loss of anthropogenic nitrogen to the environment causes many problems from increasing freshwater nitrate concentrations to raising nitrous oxide (N<sub>2</sub>O) emissions that accelerate global climate change (Duce *et al.*, 2008). A better understanding of the

structure and functioning of microbial communities involved in nitrogen transformations (such as nitrification, denitrification and nitrogen fixation) is a prerequisite to potentially counteract effects of nitrogen pollutions (Jetten, 2008).

Biochar is a carbon-rich solid produced by pyrolysis of biomass. Pyrolysis is the thermal decomposition of biomass under limited oxygen supply (Atkinson *et al.*, 2010). Biochars have a broad variety of specific physicochemical properties, which highly depend on feedstock and production temperature (Sohi *et al.*, 2010; Singh *et al.*, 2010a). Biochar produced by high-temperature pyrolysis (>550 °C) possesses a high surface area (>400 m<sup>2</sup>g<sup>-1</sup>) and a highly aromatic carbon structure, which leads to a high sorption capacity and elevated recalcitrance toward biodegradation (Joseph *et al.*, 2010; Keiluweit *et al.*, 2010; Uchimiya *et al.*, 2010). It has been shown

Correspondence: S Behrens, Geomicrobiology and Microbial Ecology, Center for Applied Geosciences, University of Tuebingen, Sigwartstraße 10, D-72076, Tuebingen, Germany.  
E-mail: sebastian.behrens@ifg.uni-tuebingen.de

<sup>4</sup>These authors contributed equally to this work.

Received 5 April 2013; revised 9 August 2013; accepted 14 August 2013; published online 26 September 2013

in several studies that biochar incorporation into soil can have diverse effects on soil quality, plant growth and greenhouse gas (GHG) emissions (Chan *et al.*, 2008; Major *et al.*, 2010; Singh *et al.*, 2010b; van Zwieten *et al.*, 2010). Biochar application to arable soil is currently heavily debated in context of soil carbon sequestration and mitigation of atmospheric CO<sub>2</sub> emissions but also as one potential strategy to reduce the release of other potent GHGs such as methane and nitrous oxide.

Nitrous oxide acts as a potent greenhouse agent in the atmosphere and represents a particular environmental problem due to its long atmospheric lifetime of 114 years. N<sub>2</sub>O is a key player in atmospheric chemical processes and represents the major source of stratospheric NO<sub>x</sub>, which acts as an ozone-depleting catalyst (Ravishankara *et al.*, 2009). Soils and oceans represent the largest sources of N<sub>2</sub>O emissions, with anthropogenic sources, such as agriculture or fossil fuel combustion, accounting for almost two-thirds of the total emissions (Denman *et al.*, 2007). The atmospheric N<sub>2</sub>O concentration of currently 319 ppb has increased by 49 ppb since the beginning of the industrial era (Forster *et al.*, 2007). The expansion of farm lands and enhanced fertilizer application are thought to increase emissions by 35–60% by 2030 (Smith *et al.*, 2007). Different microbial nitrogen-transforming processes contribute to the formation of N<sub>2</sub>O. Major sources in soils are microbial nitrification, nitrifier denitrification and heterotrophic denitrification (Wrage *et al.*, 2005). Other microbial processes that can lead to the formation of N<sub>2</sub>O are heterotrophic nitrification (Papen *et al.*, 1989; Blagodatsky *et al.*, 2006), codenitrification (Tanimoto *et al.*, 1992; Kumon *et al.*, 2002) and dissimilatory nitrate reduction to ammonia (Smith and Zimmerman, 1981; Bleakley and Tiedje, 1982; Smith, 1982, 1983). Which microbial N<sub>2</sub>O formation process dominates is largely controlled by soil geochemical conditions (Braker and Conrad, 2011). In temperate, arable soils major determinants of microbial N<sub>2</sub>O formation are oxygen partial pressure, pH, H<sub>2</sub>S concentration and the availability and speciation of nitrogen and organic carbon (Blackmer and Bremner, 1978; Sorensen *et al.*, 1980; Stevens *et al.*, 1998; Senga *et al.*, 2006; Wallenstein *et al.*, 2006; Baggs *et al.*, 2010; Cuhel *et al.*, 2010; Braker and Conrad, 2011; Philippot *et al.*, 2013).

Nitrification is the two-step oxidation of ammonium (NH<sub>4</sub><sup>+</sup>) to nitrate (NO<sub>3</sub><sup>-</sup>) via nitrite (NO<sub>2</sub><sup>-</sup>). The process is carried out by chemolithoautotrophic ammonia oxidizers and nitrite oxidizers. Ammonia-oxidizing bacteria (AOB) or archaea (AOA) oxidize NH<sub>4</sub><sup>+</sup>/NH<sub>3</sub> via the intermediate hydroxylamine (NH<sub>2</sub>OH) to NO<sub>2</sub><sup>-</sup>. The key enzyme of this process is the ammonia monooxygenase encoded by the gene *amoA*. During ammonia oxidation, N<sub>2</sub>O can be formed by chemical decomposition of NH<sub>2</sub>OH. However, levels of produced N<sub>2</sub>O are usually orders of magnitude lower (10<sup>3</sup>–10<sup>6</sup>) than those of nitrite

(Arp and Stein, 2003; Treusch *et al.*, 2005; Robertson, 2007; Canfield *et al.*, 2010; Braker and Conrad, 2011).

Denitrification is the stepwise reduction of nitrate or nitrite to N<sub>2</sub> via the intermediates NO and N<sub>2</sub>O. In contrast to nitrification, N<sub>2</sub>O is an obligate intermediate of denitrification. During denitrification, nitrate-reducers reduce nitrate to nitrite, which is further reduced by nitrite-reducing bacteria to nitric oxide (NO). The later step is catalyzed by the key enzyme nitrite reductase encoded by the genes *nirS* or *nirK*. Nitric oxide reducers convert NO to N<sub>2</sub>O, which can be the end product of denitrification or be further reduced to N<sub>2</sub> under conditions of complete denitrification. N<sub>2</sub>O reduction to N<sub>2</sub> is catalyzed by the enzyme nitrous oxide reductase encoded by the gene *nosZ* in N<sub>2</sub>O-reducing bacteria (Canfield *et al.*, 2010; Braker and Conrad, 2011). In contrast to the multiplicity of mechanisms by which N<sub>2</sub>O can be formed, N<sub>2</sub>O reduction to N<sub>2</sub> by nitrous oxide-reducing microorganisms is the only microbial sink for N<sub>2</sub>O (Thomson *et al.*, 2012).

Another important process essential to the biogeochemical cycling of nitrogen in soils is nitrogen fixation. Nitrogen fixation counteracts the loss of gaseous nitrogen to the atmosphere through microbial nitrification and denitrification by constantly replenishing the bioavailable nitrogen pool through the fixation of atmospheric N<sub>2</sub> into organic nitrogen (Jetten, 2008). The key enzyme of microbial nitrogen fixation is the highly oxygen sensitive nitrogenase encoded by the gene *nifH*.

Several studies have documented that biochar induces shifts in the microbial community composition (Rondon *et al.*, 2007; Steinbeiss *et al.*, 2009; Anderson *et al.*, 2011; Khodadad *et al.*, 2011; Ducey *et al.*, 2013), whereas other studies described that the addition of biochar to soils does affect soil N<sub>2</sub>O emissions (Yanai *et al.*, 2007; Singh *et al.*, 2010b; Taghizadeh-Toosi *et al.*, 2011; Felber *et al.*, 2012; Cayuela *et al.*, 2013). However, a potential link between the observed shifts in microbial community composition and the decreased soil N<sub>2</sub>O emissions has not been subject of systematic investigation so far.

We set up water-saturated soil microcosms with different amounts (0%, 2% and 10% w/w) of high-temperature biochar (700 °C). During a 3-month incubation experiment, we quantified N<sub>2</sub>O and CO<sub>2</sub> emissions from the soil microcosms and followed the geochemical parameters NO<sub>3</sub><sup>-</sup>, NO<sub>2</sub><sup>-</sup>, NH<sub>4</sub><sup>+</sup>, dissolved organic carbon (DOC) and pH. Besides, we determined the abundance of key functional marker genes involved in microbial nitrification, denitrification and N<sub>2</sub>-fixation (*amoA*, *nirS*, *nirK*, *nosZ* and *nifH*) by real-time PCR. The main objectives of this study were to quantify the responses of the different nitrogen-transforming functional microbial groups on soil biochar amendment and to evaluate whether alterations in the abundance and activity among the different

N-cycling functional groups might explain the reduced  $N_2O$  formation and release from soil.

## Materials and methods

### Soil sampling and biochar production

Soil samples from the top 10 cm were collected at the vineyard “Mythopia” of the Delinat Institute in Ayent (Switzerland) (46°16′4.08″N and 7°24′28.48″E). The soil is characterized as loamy sand (calcaric leptosol) with ~50% (w/w) gravel. The field moist soil was passed through a 2 mm mesh-size sieve, homogenized using a drill with a mixing blade and then stored at 4 °C in tightly closed plastic bags in the dark for less than 5 months. The biochar used in this study was produced from green waste via high-temperature pyrolysis (700 °C) by Swiss Biochar. The biochar was dried at 40 °C and only the particle size fractions between 1 mm and 2 mm were used. Soil and biochar physicochemical properties and elemental composition are summarized in Table 1 and Table S1 in the Supplementary Information.

### Experimental setup

Soil microcosms were set up in 500 ml DURAN wide neck glass bottles (Schott AG, Mainz, Germany) (Figure S1 in the Supplementary Information). Each bottle contained 202 g of field-wet soil (dry weight 180 g) or soil-biochar mixture. Three treatments with different amounts of biochar (0% (control), 2% and 10% (w/w)) were prepared. Two percent (w/w) biochar was chosen because it represents a common field application rate of 24 t ha<sup>-1</sup>. Ten percent (w/w) biochar was chosen in order to exaggerate biochar effects on soil geochemistry and microbiology. Ten percent (w/w) biochar also resembles the amounts of char found in terra preta patches (Atkinson *et al.*, 2010).

**Table 1** Physicochemical properties of the soil (calcaric leptosol) and the biochar used in this study

Parameters	Soil	Biochar
Sand (%)	44.94	ND
Silt (%)	35.37	ND
Clay (%)	19.69	ND
pH (H <sub>2</sub> O)	8.4	9.8
C <sub>tot</sub> (%)	1.87	51.90
C <sub>org</sub> (%)	0.91	48.87
N <sub>total</sub> (%)	0.17	0.59
S (%)	0.04	0.15
C:N	11	88
Particle density (g cm <sup>-3</sup> )	ND	2.0
Ash content (%)	ND	45.7
CEC (mmol <sub>c</sub> kg <sup>-1</sup> )	ND	103.4
EC (mS m <sup>-1</sup> )	ND	33.7
Total surface area (m <sup>2</sup> g <sup>-1</sup> )	ND	303

Abbreviations: CEC, cation exchange capacity; EC, electrical conductivity; ND, not determined.

The soil-biochar mixture was homogenized using a spatula and then carefully compacted by tapping the microcosms on a soft surface. All treatments were set up in duplicates. The soil microcosms were incubated open to ambient atmosphere at 28 °C in a daylight incubator. For soil geochemical and molecular analyses, duplicate soil microcosms of each treatment (a total of six bottles) were sampled destructively. Samples were taken right after microcosm setup (day 0) and after 1, 8, 15, 22, 29, 57 and 85 days of incubation. The water-filled pore space (WFPS) in the soil microcosms was adjusted to 95% in order to create water-saturated conditions similar to soil water contents in winter/spring or after a heavy rainfall. The WFPS of the microcosms was calculated according to Yanai *et al.* (2007) using a particle density of 2.00 g cm<sup>-3</sup> for the biochar and 2.65 g cm<sup>-3</sup> for the soil (Yanai *et al.*, 2007). During incubation the water content was controlled gravimetrically each week and adjusted to the initial WFPS by adding deionized water with a spray bottle. At the beginning of the experiment, the soil microcosms were fertilized with a nutrient solution containing carbon (555 mg kg<sup>-1</sup> as molasses), nitrogen (250 mg kg<sup>-1</sup> as NH<sub>4</sub>NO<sub>3</sub>), phosphorus and potassium (150 mg kg<sup>-1</sup> and 188 mg kg<sup>-1</sup> as KH<sub>2</sub>PO<sub>4</sub>). The bulk density of all three soil-biochar mixtures was determined experimentally after drying the soil for 72 h at 105 °C. The 10% (w/w) biochar microcosms had the lowest bulk density (0.99 g cm<sup>-3</sup>), followed by bottles with 2% biochar (1.10 g cm<sup>-3</sup>) and 0% biochar (1.21 g cm<sup>-3</sup>). Before subsampling for geochemical and molecular biological analyses the soil of each microcosm was transferred into a separate, clean container and thoroughly homogenized with a spatula.

### Geochemical analyses

Soil and biochar elemental composition, particle size distribution, particle density, surface area, ash and moisture content, cation exchange capacity, electrical conductivity and pH were determined according to protocols of the International Organization for Standardization. For details please refer to the Supplementary Information.

During the microcosm experiment, soil pH was determined in a 1:5 dilution with deionized water according to International Organization for Standardization 10390. For the determination of NH<sub>4</sub><sup>+</sup> and NO<sub>3</sub><sup>-</sup>, the equivalent of 5 g dry soil was mixed with 20 ml of 0.5 M K<sub>2</sub>SO<sub>4</sub> and shaken for 1 h at 130 r.p.m. (HS501, IKA, Staufen, Germany) (Singh *et al.*, 2010b). The soil solution was filtered through a 150 μm pore size cellulose filter (Whatman, Maidstone, UK) and the filtrate was again filtered through a 0.45 μm pore-size syringe filter (Millex-HA, Merck Millipore, Billerica, MA, USA). The obtained filtrate was frozen until analysis. The concentrations of NH<sub>4</sub><sup>+</sup> and NO<sub>3</sub><sup>-</sup> in the filtered solution were quantified by continuous flow



analysis (3-QuAAtro, Bran & Lübke, Nordersted, Germany). On the basis of the determined  $\text{NH}_4^+$  and  $\text{NO}_3^-$  concentrations in the soil extract  $\text{NH}_4^+$  and  $\text{NO}_3^-$  concentrations were converted to  $\text{mg NO}_3^-/\text{NH}_4^+$  per kg dry soil according to equation 1 (Eq. 1), in which  $V$  is the volume of extracting agent in L,  $m$  is the amount of dry soil in g and  $c$  is the measured concentration of  $\text{NH}_4^+$  or  $\text{NO}_3^-$   $\text{mg l}^{-1}$ .

$$C \left[ \frac{\text{mg}}{\text{kg dry soil}} \right] = \frac{c \left[ \frac{\text{mg}}{\text{L}} \right] V [\text{L}]}{m [\text{g}]} \times 1000 \quad (1)$$

Sample preparation for  $\text{NO}_2^-$  quantification was carried out as described above for  $\text{NO}_3^-/\text{NH}_4^+$ , but without the second filtration step. In order to obviate changes in nitrite concentration owing to freezing and storage,  $\text{NO}_2^-$  concentrations were analyzed spectrophotometrically directly after the extraction using a Nitrite-Test Kit (1.14776.0001, Merck, Darmstadt, Germany) according to manufacturer's instructions. For DOC, quantification sample preparation was carried out as described for  $\text{NO}_3^-/\text{NH}_4^+$  but with 40 ml 0.5 M  $\text{K}_2\text{SO}_4$  instead of 20 ml. The filtered solution was analyzed using a HighTOC analyzer (Elementar, Hanau, Germany). Both  $\text{NO}_2^-$  and DOC concentrations were also converted to  $\text{mg per kg dry soil}$  according to Equation 1.

For the determination of trace gas fluxes, the soil microcosm bottles were closed with a butyl rubber stopper before sampling. Four headspace gas samples of 25 ml were taken every hour and transferred into 22.5 ml evacuated sample vials using a gas-tight syringe (1100TLL 100.0 ml Gastight, Hamilton, Reno, NV, USA). To avoid negative pressure in the soil microcosms, a gasbag filled with  $\text{N}_2$  was connected after each sampling, which ensured a consistent ambient atmospheric pressure. The trace gas concentrations in the vials were measured using a gas chromatograph equipped with an electron capture detector ( $^{63}\text{Ni}$ -ECD) for  $\text{N}_2\text{O}$  and  $\text{CO}_2$  (Hewlett Packard, 5890 Series II). The gas chromatograph setup and configuration have been described in detail previously (Loftfield *et al.*, 1997). Gas fluxes were calculated using the slope of the temporal change in concentration of the closed bottle according to the equations published in Ruser *et al.* (1998).

#### Molecular biological analyses

In order to quantify the abundance and expression (reverse transcription) of microbial nitrogen-cycling functional marker genes, quantitative polymerase chain reaction (qPCR) was performed. Soil samples were homogenized and aliquots were stored at  $-20^\circ\text{C}$  for DNA extraction and at  $-80^\circ\text{C}$  for RNA extraction. DNA and RNA extractions were carried out in duplicates for each sample. Total DNA was extracted from 0.25 g of soil using the PowerSoil DNA Isolation Kit (MO BIO Laboratories, Carlsbad, CA, USA) with the following modifications: Bead Tubes were placed in a  $70^\circ\text{C}$  water bath for 10 min,

cooling steps were performed on ice, and before the elution step, filter tubes were incubated at room temperature for 5 min. DNA concentration and quality were determined spectrophotometrically (NanoDrop 1000, Thermo Scientific, Waltham, MA, USA), fluorometrically (Qubit 2.0 Fluorometer, Life Technologies, Carlsbad, CA, USA), and by agarose gel electrophoresis. Total RNA was isolated from 1.5 g of soil using the RNA PowerSoil Total RNA Isolation Kit (MO BIO Laboratories, Carlsbad, CA, USA) according to the manufacturer's protocol. The concentration of the extracted RNA was determined using the Qubit 2.0 Fluorometer (Life Technologies). DNA extraction efficiencies varied only slightly between different soil samples (mean DNA yield  $5.4 \pm 1.7 \mu\text{g}$  per g dry soil) and did not show any biochar-related bias. However, total RNA extraction efficiencies varied significantly between the different soil samples (mean RNA yield  $0.77 \pm 0.6 \mu\text{g}$  RNA per g dry soil). Therefore, gene transcript copy numbers were normalized to nanogram extracted RNA instead of soil dry weight. DNA digestion was performed with the Ambion TURBO DNA-free Kit (Life Technologies) with an extended incubation time of 45 min at  $37^\circ\text{C}$ . In order to assess RNA integrity, the RNA quality indicator was determined with the Experion Automated Electrophoresis Station (Bio-Rad Laboratories, Hercules, CA, USA). RNA was transcribed into complementary DNA using the SuperScript III Reverse Transcriptase (Life Technologies) according to the manufacturer's protocol. To test for the absence of residual DNA contamination in the complementary DNA preparations, we performed reverse transcription control reactions lacking reverse transcriptase enzyme. No PCR amplicons could be obtained from any sample when reverse transcriptase was omitted from the reactions.

Quantification of phylogenetic and functional marker genes (16S rRNA gene (Bacteria), *amoA* (Bacteria and Archaea), *nifH*, *nirK*, *nirS* and *nosZ*) was carried out using the SsoFast EvaGreen Supermix (Bio-Rad Laboratories, Hercules, CA, USA) and gene-specific primers. For details on plasmid standards, gene-specific qPCR primers, reaction mixtures and thermal programs, please refer to Tables S2–S4 in the Supplementary Information. Each sample was quantified in duplicates using the iCycler iQ Real-Time PCR Detection System and the iQ 5 Optical System software, version 2.0 (Bio-Rad laboratories). During qPCR setup, evaluation and data analysis, we followed the MIQE guidelines (Bustin *et al.*, 2009). For qPCR data analysis, the background subtracted raw data were exported from the iCycler system and analyzed using the Real-Time PCR Miner software (Zhao and Fernald, 2005). The algorithm calculates the efficiency (E) and threshold cycle (CT) based on the kinetics of each individual reaction. The initial template concentration N (gene copy numbers per qPCR reaction volume) was then calculated with the

following equation (Eq. (2)).

$$N = (1 + E)^{CT} \quad (2)$$

Calibration curves (log gene copy number per reaction volume versus log N) were obtained using serial dilutions of standard plasmids according to Behrens *et al.* (2008) (further details on qPCR assay validation and data analyses are given in Table S5 in the Supplementary Information). Plasmid DNA concentrations were quantified using the Qubit 2.0 Fluorometer (Life Technologies). To verify the amplification of individual PCR products and the correct amplicon size, melting curve analysis and agarose gel electrophoresis were performed. Gene copy numbers per g dry soil were calculated according to Behrens *et al.* (2008). Total bacterial cell numbers per g dry soil were calculated from the qPCR 16S rRNA gene copy numbers considering the average bacterial rRNA operon number (4.2) as derived from the Ribosomal RNA Operon Copy Number Database (<http://rrndb.mmg.msu.edu/index.php>) (Klappenbach *et al.*, 2001). Transcript copy numbers were normalized to nanogram RNA.

#### Statistical analyses

In order to identify statistically significant biochar effects, a univariate analysis of variance (ANOVA) with the 'least significant difference' *post hoc* test ( $P < 0.05$ ) was performed using the IBM SPSS Statistics 20 software package (IBM, Armonk, NY, USA). The statistical analysis was performed for each time point of sampling and for each measured parameter (geochemical and molecular). Using a univariate ANOVA, all concentration or copy number values from the control (no biochar) were individually compared with the two biochar-containing soil microcosms (2% (w/w) biochar and 10% biochar) in order to reveal differences between the control and the biochar microcosms that were statistically significant. In the provided graphs, significant differences between biochar-amended and control microcosms are indicated by lower case characters above the corresponding data points as specified in the legend of each figure.

## Results

In order to provide a better overview of the data, we only show the data of the control microcosms without biochar and the 10% (w/w) biochar microcosms here. Results of the 2% (w/w) biochar-amended microcosms in comparison with the control microcosms are given in the Supplementary Information (Supplementary Figures S2, S3). In general, the 2% and 10% biochar microcosms behaved similarly with sometimes slightly more pronounced variances and trends in comparison with the control microcosm observable for the 10% biochar microcosms. The 2% biochar data will

explicitly be mentioned when the data with respect to a 'biochar effect' were significantly different from the 10% biochar microcosms. *P*-values, otherwise explicitly stated, are given for the comparison of the control vs the 10% biochar microcosms.

#### Soil microcosm geochemical parameters

pH values were close to neutral in all microcosms and slightly increased during incubation. In the control microcosms, the pH increased from 7.2 to 7.9 and in the biochar-containing microcosms from pH 7.5 to 8.2. Overall soil pH values were significantly higher in microcosms amended with biochar than in the control microcosms over the whole course of the experiment.

We added  $250 \text{ mg kg}^{-1}$  dry soil  $\text{NH}_4\text{NO}_3$  to each microcosm at the beginning of the experiment. The amount of added  $\text{NH}_4\text{NO}_3$  corresponds to  $90 \text{ kg nitrogen ha}^{-1}$ , which is a common agricultural field application rate (Singh *et al.*, 2010b). Within the first 8 days,  $\text{NO}_3^-$  concentrations decreased rapidly from  $127.4 \pm 2.6 \text{ mg kg}^{-1}$  dry soil (control) and  $113.6 \pm 15.8 \text{ mg kg}^{-1}$  dry soil (10% (w/w) biochar) to  $1.2 \pm 0.06 \text{ mg kg}^{-1}$  dry soil and  $2.7 \pm 0.02 \text{ mg kg}^{-1}$  dry soil, respectively (Figure 1a). From day 8 to day 85, nitrate concentrations stayed below  $3.7 \pm 0.3 \text{ mg kg}^{-1}$  dry soil in all treatments (Figure 1a). Only at day 1, nitrate concentrations were significantly lower ( $P = 0.002$ ) in the 10% biochar microcosms compared with the control microcosm (Figure 1a), whereas from day 8 to day 85, nitrate concentrations were always slightly higher ( $P < 0.038$ ) in the 10% biochar microcosms than in the control microcosms.

Compared with the nitrate concentrations, ammonia concentrations decreased more slowly but constantly with time reaching concentrations of  $7.7 \pm 1.0$  (control) and  $12.5 \pm 0.3$  (10% biochar)  $\text{mg kg}^{-1}$  dry soil at day 85 (Figure 1a). Only at day 8, ammonia concentrations were significantly lower in the 10% biochar microcosms ( $P = 0.014$ ), whereas from day 29 to day 85 they were significantly higher in the 10% biochar microcosms compared with the control microcosms ( $P < 0.029$ ) (Figure 1a).

Nitrite concentrations were highest at day 1 in the biochar and in the control microcosms ( $37.7 \pm 2.7 \text{ mg kg}^{-1}$  dry soil and  $52.4 \pm 2.1 \text{ mg kg}^{-1}$  dry soil, respectively) (Figure 1b). ANOVA revealed that the higher nitrite concentrations in the control compared with the biochar microcosms at day 1 were statistically significant ( $P = 0.016$ ) (Figure 1b). Corresponding to the nitrate and the nitrite data, the highest  $\text{N}_2\text{O}$  fluxes were recorded during the first week (until day 8) in all three treatments (control, 2%, and 10% biochar). At day 1,  $\text{N}_2\text{O}$  fluxes were significantly higher in the control microcosms without biochar ( $5631 \pm 766 \mu\text{g N}_2\text{O-N m}^{-2} \text{ h}^{-1}$ ) compared with the biochar-containing microcosms ( $175 \pm 116 \mu\text{g N}_2\text{O-N m}^{-2} \text{ h}^{-1}$  in the 10%

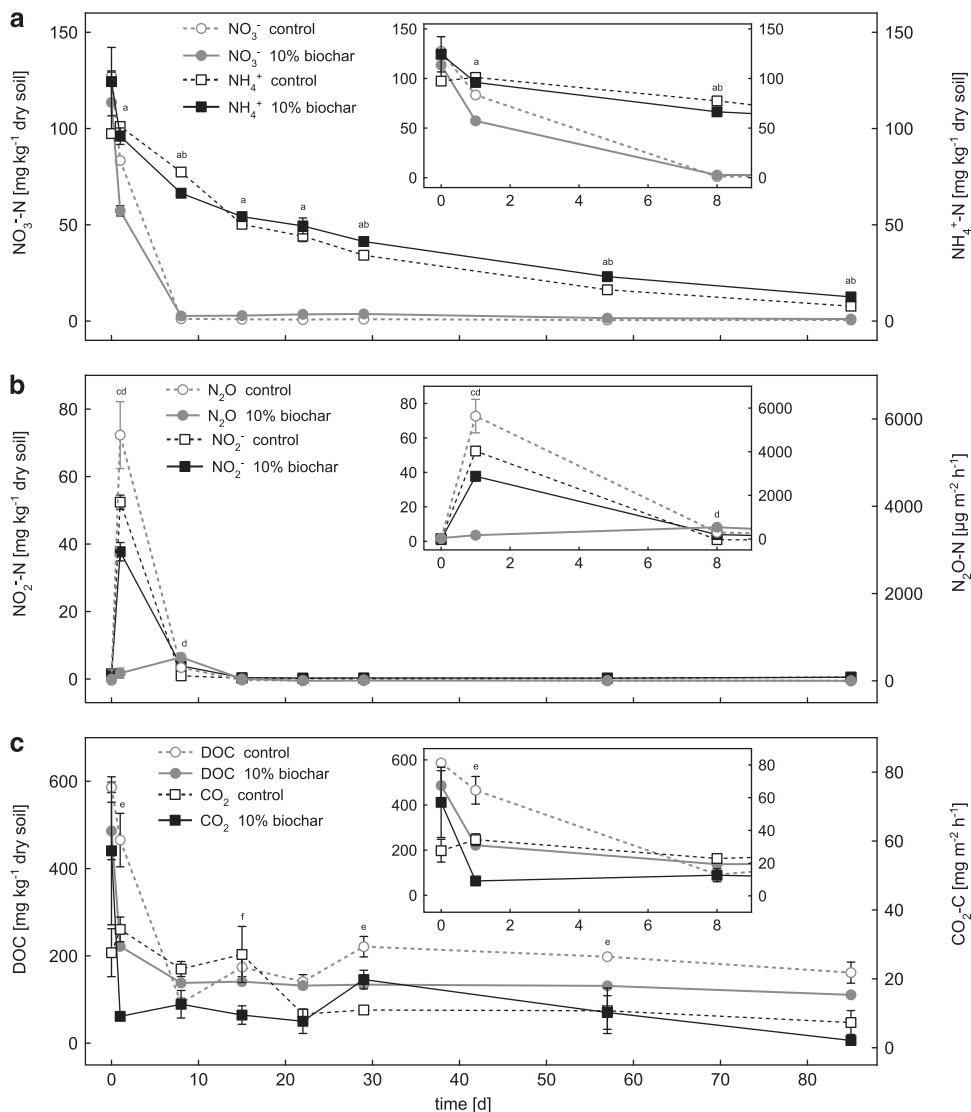


**Figure 1** Change in nitrogen (a, b) and carbon (c) geochemical parameters in the control and 10% (w/w) biochar-containing soil microcosms over time. Panels a, b show changes in the concentrations of nitrate, nitrite, ammonium and nitrous oxide, whereas panel c shows the DOC and carbon dioxide data. The small inserted graphs show a magnified view of the data for the first 8 days. Open symbols with dashed lines represent data of the control microcosms without biochar. Filled symbols with solid lines represent data of the soil microcosms with 10% (w/w) biochar. Statistically significant differences (univariate ANOVA, *post hoc*: least significant difference) between control and 10% (w/w) biochar microcosms at a certain time point are indicated by lower-case letters above the individual data points (a = NO<sub>3</sub><sup>-</sup>, b = NH<sub>4</sub><sup>+</sup>, c = N<sub>2</sub>O, d = NO<sub>2</sub><sup>-</sup>, e = DOC, f = CO<sub>2</sub>).

biochar-containing and  $2969 \pm 554 \mu\text{g N}_2\text{O-N m}^{-2} \text{h}^{-1}$  in the 2% biochar-containing microcosms) ( $P=0.002$  and  $0.017$ , respectively) (Figure 1b and Supplementary Figure S2b). After day 1, N<sub>2</sub>O fluxes decreased strongly to  $<500 \mu\text{g N}_2\text{O-N m}^{-2} \text{h}^{-1}$  at day 8 and  $<50 \mu\text{g N}_2\text{O-N m}^{-2} \text{h}^{-1}$  from day 15 to day 85 in all three treatments (Figure 1b and Supplementary Figure S2b).

Initial DOC concentrations resembled the amount of DOC added in form of molasses at the beginning of the experiment ( $555 \text{ mg kg}^{-1}$  dry soil). DOC concentrations decreased rapidly within the first week in all setups leveling off at an average concentration of  $119.6 \pm 22.0 \text{ mg kg}^{-1}$  dry soil at day 8 (Figure 1c). As can be seen in Figure 1c, the

10% biochar-containing microcosms showed significantly lower DOC concentrations compared with the control at day 1 ( $P=0.018$ ) and between day 29 and day 57 ( $P<0.023$ ).

CO<sub>2</sub> fluxes decreased from  $57.2 \pm 21.5 \text{ mg m}^{-2} \text{h}^{-1}$  to  $12.6 \pm 4.0 \text{ mg m}^{-2} \text{h}^{-1}$  during the first day of incubation in the 10% biochar microcosms (Figure 1c). Initial CO<sub>2</sub> fluxes in the control microcosm were lower than in the biochar microcosms ( $27.6 \pm 7.0 \text{ mg m}^{-2} \text{h}^{-1}$ ) and further decreased to  $9.8 \pm 0.5 \text{ mg m}^{-2} \text{h}^{-1}$  after day 22 (Figure 1c). However, according to the ANOVA, CO<sub>2</sub> fluxes showed no significant differences between biochar-containing and control microcosms throughout the whole course of the experiment (Figure 1c)

except for day 15 when significantly higher CO<sub>2</sub> emissions from the control microcosms were measured ( $P = 0.039$ ).

#### Abundance of 16S rRNA and N-cycling functional marker genes

As shown in Figure 2a, total bacterial abundance increased temporarily during the beginning of the experiment reaching a maximum of  $2.8 \times 10^{10}$  gene copies per g dry soil at day 8. Afterwards, bacterial 16S rRNA gene copy numbers slowly returned to initial values of  $5.5 \times 10^9$  gene copies per g dry soil.

The statistical analysis revealed no significant differences between control and biochar-containing soil microcosms with respect to total bacterial 16S rRNA gene copy numbers.

The abundance of bacteria capable of fixing nitrogen was determined by quantification of *nifH* gene copy numbers. In accordance to 16S rRNA gene copy numbers, *nifH* gene copy numbers increased rapidly within the first 8 days reaching a maximum of  $1.7 \times 10^{10}$  gene copies per g dry soil (Figure 2a) at day 8. Between day 8 and day 29, *nifH* gene copies slightly fluctuated before they remained quite constant from day 29 to 85 reaching final gene

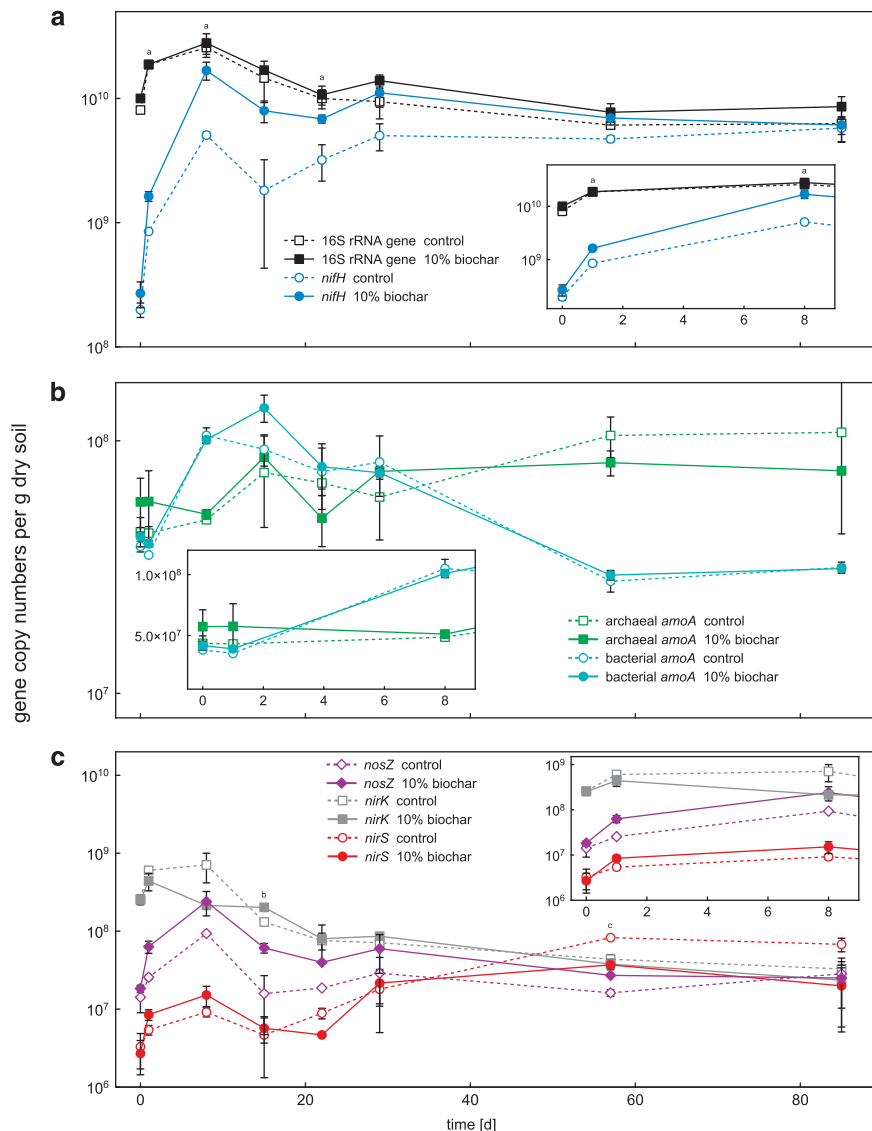


**Figure 2** Gene copy numbers per gram dry soil over time for various key genes of microbial nitrogen transformation processes in the control and 10% (w/w) biochar-containing microcosms. Panel a shows changes in total bacterial 16S rRNA and *nifH* gene copy numbers. In panel b, archaeal and bacterial *amoA* gene copy numbers are shown. Panel c summarizes the gene copy data for *nirS*, *nirK* and *nosZ*. The small inserted graphs show a magnified view of the data for the first 8 days. Note that the y axes of the inserted graphs in panels a, b and c have a slightly different scale from the corresponding overview graphs. Open symbols with dashed lines represent data measured in the control microcosms without biochar. Filled symbols with solid lines represent data of the soil microcosms with 10% (w/w) biochar. Statistically significant differences (univariate ANOVA, *post hoc*: least significant difference) between control and 10% (w/w) biochar microcosms at a certain time point are indicated by lower-case letters above the individual data points (a = *nifH*, b = *nosZ* and c = *nirS*).



counts close to the total copy number of bacterial 16S rRNA genes (control microcosms:  $5.8 \times 10^9$  gene copies per g dry soil; 10% (w/w) biochar-containing microcosms:  $6.1 \times 10^9$  gene copies per g dry soil; 2% biochar-containing microcosms:  $6.8 \times 10^9$  gene copies per g dry soil) (Figure 2a and Supplementary Figure S3a). Over the whole incubation period, *nifH* gene copy numbers were consistently higher in the biochar-containing microcosms compared with the control microcosms with significantly higher values at day 1 ( $P=0.031$ ), 8 ( $P=0.018$ ) and 22 ( $P=0.031$ ) (Figure 2a).

The abundance of AOA and AOB was quantified by determining archaeal and bacterial *amoA* gene copy numbers. Archaeal *amoA* gene copies fluctuated within the first month between  $4.3 \times 10^7$  and  $8.6 \times 10^7$  gene copies per g dry soil in the control and the 10% biochar-containing microcosms. From day 22 to day 85, archaeal *amoA* gene copies increased from  $6.8 \times 10^7$  to  $1.1 \times 10^8$  gene copies per g dry soil in the control microcosms and from  $5.0 \times 10^7$  to  $7.6 \times 10^7$  gene copies per g dry soil in the 10% biochar microcosms (Figure 2b). Bacterial *amoA* gene copies increased from  $3.8 \times 10^7$  to  $1.1 \times 10^8$  gene copies per g dry soil at day 8 in the control microcosms and from  $4.2 \times 10^7$  to  $1.4 \times 10^8$  gene copies per g dry soil at day 15 in the 10% biochar microcosms. After the initial increase, bacterial *amoA* gene copies decreased toward the end of the incubation period (day 85) in both control and biochar microcosms reaching  $3.2 \times 10^7$  and  $3.1 \times 10^7$  gene copies per g dry soil, respectively (Figure 2b). ANOVA revealed no significant differences between control and biochar-amended microcosms (2% and 10% biochar) for the archaeal and bacterial *amoA* gene data.

Nitrite-reducing bacteria were quantified by determining the copy numbers of *nirS* and *nirK* per g dry soil in each microcosm. As shown in Figure 2c, initial *nirS* gene copy numbers were two orders of magnitude lower ( $3.0 \times 10^6$ ) than *nirK* gene copy numbers ( $2.0 \times 10^8$ ); however, over the course of the experiment, *nirS* and *nirK* gene copy numbers approximated. *nirK* gene copy numbers decreased, whereas *nirS* gene copy numbers increased. After 85 days, *nirS* gene copy numbers even outnumbered *nirK* gene copy numbers, as *nirS* increased to  $4.4 \times 10^7$  gene copies per g dry soil and *nirK* decreased to  $2.8 \times 10^7$  gene copies per g dry soil (Figure 2c).

Differences between the biochar and the control microcosms with respect to nitrite-reductase gene copy numbers were most of the time not significant based on ANOVA. Only at day 57, *nirS* gene copy numbers were significantly higher in the control microcosms than in the 10% (w/w) biochar-containing microcosms ( $P=0.0009$ ) (Figure 2c).

The abundance of nitrous oxide-reducing bacteria was followed by quantifying *nosZ* gene copy numbers. *nosZ* gene copy numbers initially increased from  $1.4 \times 10^7$  to  $9.3 \times 10^7$  gene copies

per g dry soil (control microcosms) and from  $1.8 \times 10^7$  to  $2.4 \times 10^8$  gene copies per g dry soil (10% biochar) toward day 8. Thereafter, *nosZ* gene copy numbers decreased and reached  $2.8 \times 10^7$  gene copies per g dry soil in the control microcosms and  $2.5 \times 10^7$  gene copies per g dry soil in the 10% biochar-containing microcosms at the end of the experiment (Figure 2c). Significantly higher *nosZ* gene copy numbers in biochar-containing compared to control microcosms were quantified at day 15 ( $P=0.042$ ) (Figure 2c).

#### Functional gene ratios and *nosZ* gene transcript abundance

As shown in Figure 3a, the ratio of *nosZ* gene copies over the sum of *nirS* and *nirK* gene copies ( $nosZ/(nirS + nirK)$ ) was strongly affected by biochar addition and was always higher in the biochar-containing microcosms compared with the control microcosms throughout the entire experiment. A  $nosZ/(nirS + nirK)$  ratio of 1 means equal copy numbers of nitrite and nitrous oxide reductase genes per g dry soil. In the biochar-containing microcosms, the ratio reached 1 at day 8 shortly after the greatest differences in  $N_2O$  emissions between the control and biochar-containing microcosms have been quantified ( $P=0.002$ ) (Figure 3a). Statistical analysis confirmed significantly higher  $nosZ/(nirS + nirK)$  ratios in the 10% (w/w) biochar-containing microcosms compared with the control microcosms at day 1, ( $P=0.023$ ), 8 ( $P=0.044$ ) and at day 57 ( $P=0.013$ ) (Figure 3a).

As shown in Figure 3b, the ratio of archaeal *amoA* gene copies over bacterial *amoA* gene copies only slightly changed between day 1 and day 29 (values from 0.5 to 1.5). After day 29, the AOA/AOB ratio increased to 2.8 and 3.8 in biochar-containing and control microcosms, respectively, independent of biochar addition (Figure 3b).

The relative abundance of *nifH* gene copies (*nifH* gene copies over bacterial 16S rRNA gene copies) increased in the control microcosms from  $2.5 \pm 0.4\%$  to  $94.2 \pm 7.5\%$  at day 85 (Figure 3c). In the 10% biochar-containing microcosms, the relative abundance of *nifH* gene copies increased from  $2.7 \pm 0.6\%$  to  $90.8 \pm 4.8\%$  at day 57 (Figure 3c). Until day 85 the relative abundance of *nifH* gene copies then decreased to  $71.8 \pm 2.9\%$  in the 10% biochar-containing microcosms. Significantly higher *nifH*/16S rRNA gene ratios in biochar-containing microcosms compared with the control microcosms were statistically confirmed for day 1, 8, 15, 22 and day 85 ( $P<0.043$ ) (Figure 3c).

As shown in Figure 4, the number of *nosZ* gene transcripts was about sixfold higher in the 10% biochar microcosms compared with the control microcosms at day 1. Gene transcript copy numbers were strongly affected by biochar addition and increased from  $1.1 \times 10^4$  to  $1.8 \times 10^4$  *nosZ* gene transcripts per ng RNA in the 10%



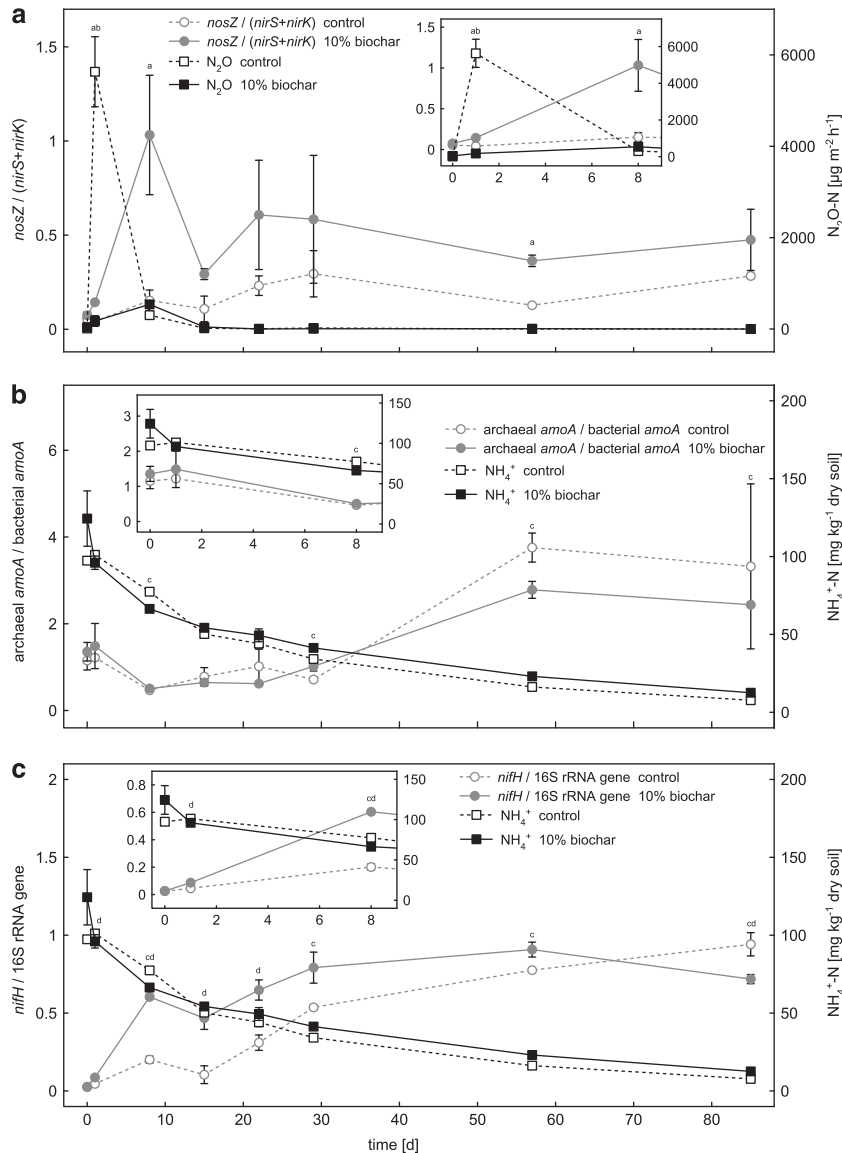


**Figure 3** Changes in gene ratios or relative gene abundances plotted together with selected geochemical parameters of the control and 10% (w/w) biochar-containing soil microcosms over time. Panel **a** shows  $N_2O$  emissions in comparison with the ratio of *nosZ* over the sum of *nirS* and *nirK* gene copy numbers (*nosZ*/(*nirS* + *nirK*)). In panel **b**, ammonium concentrations are plotted together with the ratio of AOA over AOB (AOA/AOB ratio) as calculated from the bacterial and archaeal *amoA* gene copies numbers. Panel **c** shows ammonium concentrations and the relative abundance of *nifH* genes over total bacterial 16S rRNA genes. The small inserted graphs show a magnified view of the data for the first 8 days. Note that the y axes of the inserted graphs in panels **b** and **c** have a slightly different scale from the corresponding overview graphs. Open symbols with dashed lines represent data measured in the control microcosms without biochar. Filled symbols with solid lines represent data of the soil microcosms with 10% (w/w) biochar. Statistically significant differences (univariate ANOVA, *post hoc*: least significant difference) between control and 10% (w/w) biochar microcosms at a certain time point are indicated by lower-case characters above the individual data points (a = *nosZ*/(*nirS* + *nirK*), b =  $N_2O$ , c =  $NH_4^+$  and d = *nifH*/bacterial 16S rRNA genes).

biochar-containing microcosms between day 0 and day 1 (Figure 4). In contrast, in the control microcosms without biochar *nosZ* gene transcripts per ng RNA decreased from  $0.7 \times 10^4$  to  $0.3 \times 10^4$  in the same period, what resulted in significantly higher *nosZ* transcript copy numbers in the 10% biochar-containing microcosms compared with the control microcosms at day 1 ( $P=0.03$ ). Notably,  $N_2O$  emissions were inversely correlated to the *nosZ* transcript copy numbers (highest in the control microcosms and significantly lower in the

biochar-containing microcosms ( $P=0.002$ )) at day 1 (Figure 1b, Supplementary Figure S2b).

## Discussion

### Geochemistry of the microcosms

At the beginning of the experiments all soil microcosms were amended with  $NH_4NO_3$ ,  $KH_2PO_4$ , and molasses at typical field application rates (N:  $90 \text{ kg ha}^{-1}$ , P:  $50 \text{ kg ha}^{-1}$ , K:  $63 \text{ kg ha}^{-1}$ ) in order

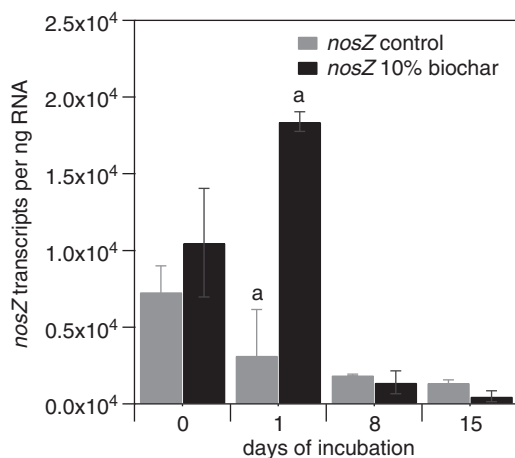


**Figure 4** *nosZ* transcript copy numbers per ng RNA in the control microcosms and in the soil microcosms with 10% (w/w) biochar during the initial 15 days of incubation. Gray bars represent data measured in the control microcosms without biochar. Black bars represent data of the soil microcosms with 10% (w/w) biochar. Statistically significant differences between 10% (w/w) biochar-containing and control microcosms are indicated by the letter 'a' above the respective time points.

to simulate a fertilization event and prevent carbon limitation (Singh *et al.*, 2010b). Because our soil microcosms were plant-free and the soil contained little plant material, we added molasses as a carbon source to create a situation when larger quantities of plant-derived carbon become available, for example, after a cut or heavy rainfall (Felber *et al.*, 2012).

The observed rapid decrease in DOC in all microcosms corresponded to the quantified CO<sub>2</sub> formation rates at the beginning of incubation suggesting that in general biochar addition did not impair carbon-based microbial respiration (Figure 1c). Furthermore, the decrease in DOC within the first week until day 8 correlated well to the increase in total bacterial 16S rRNA gene copy numbers in all microcosms ( $R^2 = 0.79$ ) (Figures 1c, 2a), indicating that the oxidation of readily available organic carbon stimulated microbial growth in the soil microcosms.

The succession of NH<sub>4</sub><sup>+</sup> and NO<sub>3</sub><sup>-</sup> concentrations in the soil microcosms confirmed the expected predominance of anoxic conditions in the water-saturated soil microcosms (WFPS 95%). Rapidly decreasing NO<sub>3</sub><sup>-</sup> concentrations suggests that denitrification prevailed under these conditions (Figure 1a). Evidence for the occurrence of NO<sub>3</sub><sup>-</sup> reduction was also provided by the intermittent accumulation of NO<sub>2</sub><sup>-</sup> within the first week (Figure 1b) (Lam and Kuypers, 2011). Slowly decreasing NH<sub>4</sub><sup>+</sup> concentrations could either be due to NH<sub>4</sub><sup>+</sup> assimilation or due to low levels of either aerobic or anaerobic ammonia oxidation caused by oxygen diffusion into the top layers of the soil microcosms or by oxidation of NH<sub>4</sub><sup>+</sup> with NO<sub>2</sub><sup>-</sup> or an alternative electron acceptor such as iron (Lam and Kuypers, 2011; Yang *et al.*, 2012).

N<sub>2</sub>O emissions from soil were highest at day 1 and hence most likely a direct consequence of the initial fertilizer application and soil moisture adjustment (Figure 1b). As NH<sub>4</sub><sup>+</sup>, NO<sub>3</sub><sup>-</sup> and DOC concentrations decreased N<sub>2</sub>O fluxes declined in all microcosms because electron donors and acceptors for microbial N<sub>2</sub>O formation became limiting. The significantly lower N<sub>2</sub>O emissions from biochar-containing microcosms observed within the first week (Figure 1b, Supplementary Figure S2b) agree with the findings of several recently published field- and laboratory-based studies using different biochars and soils (Yanai *et al.*, 2007; Singh *et al.*, 2010b; van Zwieten *et al.*, 2010; Taghizadeh-Toosi *et al.*, 2011; Wang *et al.*, 2011b; Augustenborg *et al.*, 2012; Wang *et al.*, 2012; Zheng *et al.*, 2012; Zhang *et al.*, 2012a, b). According to these studies, the most important environmental factors responsible for the reduced N<sub>2</sub>O emissions from biochar-amended soil were: (i) limited bioavailability of electron donors and acceptors (DOC, NO<sub>3</sub><sup>-</sup> and NH<sub>4</sub><sup>+</sup>) for microbial nitrification and denitrification due to sorption/immobilization onto biochar particles (Singh *et al.*, 2010b; Taghizadeh-Toosi *et al.*, 2011; Wang *et al.*, 2011a); (ii) improved soil aeration through biochar addition and consequently reduced denitrification (Yanai *et al.*, 2007; van Zwieten *et al.*, 2010; Augustenborg *et al.*, 2012; Zhang *et al.*, 2012b); and (iii) increased activity of N<sub>2</sub>O-reducing bacteria due to an elevated soil pH caused by biochar addition (van Zwieten *et al.*, 2010; Zheng *et al.*, 2012).

#### 16S rRNA and N-cycling functional marker genes

**Ammonia oxidation.** In accordance with Ducey *et al.* (2013), no significant correlation between the abundance of AOA and AOB and soil biochar amendment was found in this study (Figure 2b). However, independent of the amount of biochar added the AOA/AOB gene ratio increased over time in all microcosms (Figure 3b).

**N<sub>2</sub> fixation.** Soil biochar amendment alters several environmental parameters known to affect the abundance and activity of N<sub>2</sub>-fixing bacteria, such as oxygen availability, pH, C:N ratio and nitrogen availability (Reed *et al.*, 2007; Hsu and Buckley, 2008; Atkinson *et al.*, 2010; Singh *et al.*, 2010a). It is therefore most likely that the interplay of multiple of these parameters might be responsible for the elevated *nifH* gene copy numbers in the biochar-containing microcosms (Figure 2a). The biochar-containing microcosms had a slightly elevated pH ( $\leq 0.3$  pH units) and slightly lower concentrations of K<sub>2</sub>SO<sub>4</sub>-extractable NO<sub>3</sub><sup>-</sup> and NH<sub>4</sub><sup>+</sup> (statistically significant only at individual time points) compared with the control microcosms.

Cusack *et al.* (2009) found a positive correlation between biological nitrogen fixation and forest soil

C:N ratio in tropical and lower montane rainforests. Even though high-temperature pyrolysis biochar is highly stable and mostly recalcitrant toward microbial degradation (Joseph *et al.*, 2010) many soil microorganisms are capable of degrading aromatic carbon structures when other more readily available carbon sources become limiting. The biochar used in this study had a C:N ratio of 88, whereas the C:N ratio of the soil was 11 (Table 1). Assimilation and biomass synthesis from biochar-carbon therefore required an additional source of nitrogen what might favor microorganisms capable of nitrogen fixation when alternative organic and inorganic nitrogen sources became limiting or non-bioavailable with time.

**Denitrification.** Net N<sub>2</sub>O formation and release from soils have been shown to be strongly linked to the abundance and activity of N<sub>2</sub>O-reducing bacteria as the only biotic sink of N<sub>2</sub>O in the environment (Thomson *et al.*, 2012). Philippot *et al.* (2011) showed that one-third of all denitrifiers, defined as *nirS*- or *nirK*-containing microorganisms (Jones *et al.*, 2008), lack the genetic potential for N<sub>2</sub>O reduction and thus are major contributors to microbial N<sub>2</sub>O production (Philippot *et al.*, 2011). Our data suggest that the addition of biochar changed the denitrifier microbial community composition by promoting the growth (Figure 3a) and activity of N<sub>2</sub>O-reducing bacteria (containing a *nosZ* gene) (Figure 4) relative to *nirS*- and *nirK*-containing denitrifiers. By this our findings support the hypothesis of Anderson *et al.* (2011) who suggested that decreased N<sub>2</sub>O emissions from biochar-amended soil might be caused by an enhanced growth and activity of microorganisms capable of complete denitrification (Anderson *et al.*, 2011).

The incorporation of biochar into soil alters various geochemical soil parameters which are known to affect the diversity, abundance and functioning of N<sub>2</sub>O-producing microbial communities in soils and thereby soil N<sub>2</sub>O emissions, such as nitrogen speciation (NO<sub>3</sub><sup>-</sup>/NH<sub>4</sub><sup>+</sup>) and availability, pH and oxygen saturation (Richardson *et al.*, 2009; Braker and Conrad, 2011). Singh *et al.* (2010b) argued that over time the addition of biochar to soils increases sorption of inorganic nitrogen compounds such as NH<sub>4</sub><sup>+</sup> and NO<sub>3</sub><sup>-</sup> to the soil matrix which decreases their availability for microbial N<sub>2</sub>O production. We cannot exclude that biochar aging and associated changes in its cation exchange capacity might have affected NO<sub>3</sub><sup>-</sup> sorption during the 3 months of incubation (Singh *et al.*, 2010b), but the observed reduction of N<sub>2</sub>O emissions occurred within the first week of incubation (Figure 3a) and the fresh biochar used in this study showed little to no NO<sub>3</sub><sup>-</sup> and NH<sub>4</sub><sup>+</sup> sorption in preliminary experiments (Supplementary Figure S4).

Bergaust *et al.* (2010) reported that soil pH exerts a strong control on the N<sub>2</sub>O/N<sub>2</sub> product ratio in soils

(high ratios at low pH), because at a pH below 7 N<sub>2</sub>O reductase synthesis and assembly are inhibited. As in our experiments the pH in the presence of biochar increased  $\leq 0.3$  pH units and the soil pH was rather alkaline (pH 8.4), the observed decrease in N<sub>2</sub>O emission are unlikely to be caused by post-translational effects on N<sub>2</sub>O reductase folding and inhibition.

Van Zwieten *et al.* (2009) postulated that biochar amendment can create anoxic microsites within soil particles and aggregates, for example, through the promotion of heterotrophic microbial respiration and growth on the surface of biochar particles which leads to local anaerobiosis. The formation of anoxic microsites would enhance complete versus incomplete denitrification by stimulating growth and activity of N<sub>2</sub>O-reducing microorganisms, because N<sub>2</sub>O reductases have been reported to be more sensitive to O<sub>2</sub> than enzymes involved in N<sub>2</sub>O formation (Betlach and Tiedje, 1981; Jungkunst *et al.*, 2006). This might in particular be relevant for well-aerated soils and would generally not apply to water-saturated conditions as present in our microcosm experiment. However, as oxygen diffusion into the top soil layers of our microcosms was possible because the microcosms were incubated under ambient atmosphere, biochar addition might have contributed to the formation of more anoxic microsites in the top layers of the soil microcosms. Further evidence for a potentially lower oxygen availability in the biochar-containing microcosms also comes from the elevated *nifH* gene copy numbers in the microcosms because a low oxygen partial pressure is also considered to be one of the controlling factors of microbial N<sub>2</sub>-fixation (Vitousek *et al.*, 2002; Reed *et al.*, 2011) (Figure 3c).

A recent study by Cayuela *et al.* (2013) using 15 agricultural soils showed that biochar consistently reduced the N<sub>2</sub>O/(N<sub>2</sub>+N<sub>2</sub>O) ratio, which demonstrated that soil biochar amendment promoted the last step of denitrification. According to Cayuela *et al.* (2013) biochar can function as an 'electron shuttle' facilitating the transfer of electrons to soil denitrifying microorganisms. Taken together with its acid buffer capacity and its high surface area, the electron shuttling properties of biochar would promote the reduction of N<sub>2</sub>O to N<sub>2</sub>. The increased abundance and gene expression activity of *nosZ*-containing microorganisms observed in this study might be one explanation for the decreased ratio of N<sub>2</sub>O/(N<sub>2</sub>+N<sub>2</sub>O) observed by Cayuela *et al.* (2013).

**Conclusions and implications.** The N<sub>2</sub>O fluxes quantified in this study agree with the N<sub>2</sub>O fluxes previously quantified in water-saturated (WFPS > 70%) soil microcosms, flow-through columns or field sites after the application of high doses of fertilizers (Flessa *et al.*, 1995; Clayton *et al.*, 1997; Flessa *et al.*, 1998; Flechard *et al.*, 2005; Ruser *et al.*, 2006; Yanai *et al.*, 2007; van Zwieten *et al.*, 2010;

Singh *et al.*, 2010b). The added carbon in form of molasses thereby created a situation with high microbial activity, comparable to field situations when larger quantities of residues become available such as after a cut, during the winter/spring season when freeze-thaw cycles occur or after heavy rainfalls (Felber *et al.*, 2012). According to our data, N<sub>2</sub>O emission peaks in water-saturated soils after fertilizer application may be reduced by up to 96% in the presence of 120 t ha<sup>-1</sup> biochar (10% (w/w) biochar) and up to 47% in the presence of 24 t ha<sup>-1</sup> biochar (2% w/w biochar) if the magnitude of the biochar effect in the lab is similar in the field. However, one needs to take into account that under field conditions emissions are usually less pronounced because most of the soil organic matter or plant residues are not readily biodegradable and first need to be broken down into monomers in order to effectively stimulate microbial N<sub>2</sub>O production activity. Furthermore, typical biochar application rates are in the range of 5 to 50 t ha<sup>-1</sup>. So assuming a potential N<sub>2</sub>O emission reduction of about 47% as observed for the 2% (w/w) biochar-containing microcosms seems to be a more realistic and economic scenario and is in good agreement with results from other laboratory and field studies that reported reduction of N<sub>2</sub>O emissions by 50–80% (Lehmann and Joseph, 2009; Singh *et al.*, 2010b; van Zwieten *et al.*, 2010; Taghizadeh-Toosi *et al.*, 2011; Zhang *et al.*, 2012a). However, the general impact of our findings needs additional evaluation and it would be a far stretch to extrapolate our results directly to field emissions because (i) only one soil and one biochar have been used, (ii) the impact of biochar on the microbial community of nitrogen-transforming microorganisms might vary considerably depending on soil and biochar type, (iii) N<sub>2</sub> formation has not been quantified and (iv) only a relative short time period of 3 months has been considered in the experiments presented here. Nonetheless, the documented changes in the relative abundance of N<sub>2</sub>O-forming and reducing microorganisms and the changes in *nosZ* gene expression provide (i) new mechanistic insights into the effect of biochar on the structure and functioning of the denitrifying soil microbial community; and (ii) offer a tentative explanation for the observed reduction of N<sub>2</sub>O emissions caused by soil biochar amendment as an increased abundance and gene expression activity of *nosZ*-containing microorganisms might enhance the direct microbial reduction of N<sub>2</sub>O to N<sub>2</sub> thereby decreasing net soil N<sub>2</sub>O release.

In order to confirm the findings of this study and further advance our understanding on the impact of biochar on the nitrogen cycling microbial community and soil N<sub>2</sub>O emissions, field studies with different biochars over longer time periods are needed. Furthermore, two recent studies revealed a physiological dichotomy in the diversity of N<sub>2</sub>O-reducing microorganisms (Sanford *et al.*, 2012; Jones *et al.*, 2013). These recent findings

might also be of importance for understanding the relationship between N<sub>2</sub>O reduction and the activity and diversity of N<sub>2</sub>O-reducing microorganisms in biochar-amended soils and should be taken into account in future studies.

## Conflict of Interest

The authors declare no conflict of interest.

## Acknowledgements

We thank Hans-Peter Schmidt of the Delinat Institute for Ecology und Climate Farming (Ayent, Switzerland) for providing soil and biochar, Elizaveta Krol (Center for Biological Systems Analysis, University of Freiburg, Germany) for providing the strain *Ensifer melilotii* 1021, Stefanie Töwe (Helmholtz Zentrum München: Research Unit Environmental Genomics, Germany) for providing archaeal and bacterial *amoA* standard plasmids for qPCR and Sven Marhan (Institute of Soil Science and Land Evaluation, University of Hohenheim, Germany) for helpful discussions. We are also grateful for the technical support of Ellen Struve, Karin Stögerer and Bernice Nisch.

## References

- Anderson CR, Condron LM, Clough TJ, Fiers M, Stewart A, Hill RA *et al.* (2011). Biochar induced soil microbial community change: implications for biogeochemical cycling of carbon, nitrogen and phosphorus. *Pedobiologia* **54**: 309–320.
- Arp DJ, Stein LY. (2003). Metabolism of inorganic N compounds by ammonia-oxidizing bacteria. *Crit Rev Biochem Mol Biol* **38**: 471–495.
- Atkinson CJ, Fitzgerald JD, Hipps NA. (2010). Potential mechanisms for achieving agricultural benefits from biochar application to temperate soils: a review. *Plant Soil* **337**: 1–18.
- Augustenborg CA, Hepp S, Kammann C, Hagan D, Schmidt O, Muller C. (2012). Biochar and earthworm effects on soil nitrous oxide and carbon dioxide emissions. *J Environ Qual* **41**: 1203–1209.
- Baggs EM, Smales CL, Bateman EJ. (2010). Changing pH shifts the microbial source as well as the magnitude of N<sub>2</sub>O emission from soil. *Biol Fert Soils* **46**: 793–805.
- Behrens S, Azizian MF, McMurdie PJ, Sabalowsky A, Dolan ME, Semprini L *et al.* (2008). Monitoring abundance and expression of "*Dehalococcoides*" species chloroethene-reductive dehalogenases in a tetrachloroethene-dechlorinating flow column. *Appl Environ Microbiol* **74**: 5695–5703.
- Bergaust L, Mao Y, Bakken LR, Frostegard A. (2010). Denitrification response patterns during the transition to anoxic respiration and posttranscriptional effects of suboptimal pH on nitrogen oxide reductase in *Paracoccus denitrificans*. *Appl Environ Microbiol* **76**: 6387–6396.
- Betlach MR, Tiedje JM. (1981). Kinetic explanation for accumulation of nitrite, nitric oxide, and nitrous oxide during bacterial denitrification. *Appl Environ Microbiol* **42**: 1074–1084.



- Blackmer AM, Bremner JM. (1978). Inhibitory effect of nitrate on reduction of  $N_2O$  to  $N_2$  by soil microorganisms. *Soil Biol Biochem* **10**: 187–191.
- Blagodatsky SA, Kesik M, Papen H, Butterbach-Bahl K. (2006). Production of NO and  $N_2O$  by the heterotrophic nitrifier *Alcaligenes faecalis* parafaecalis under varying conditions of oxygen saturation. *Geomicrobiol J* **23**: 165–176.
- Bleakley BH, Tiedje JM. (1982). Nitrous oxide production by organisms other than nitrifiers and denitrifiers. *Appl Environ Microbiol* **44**: 1342–1348.
- Braker G, Conrad R. (2011). Diversity, structure, and size of  $N_2O$ -producing microbial communities in soils—What matters for their functioning? *Adv Appl Microbiol* **75**: 33–70.
- Bustin SA, Benes V, Garson JA, Hellems J, Huggett J, Kubista M *et al.* (2009). The MIQE guidelines: Minimum information for publication of quantitative real-time PCR experiments. *Clin Chem* **55**: 611–622.
- Canfield DE, Glazer AN, Falkowski PG. (2010). The evolution and future of Earth's nitrogen cycle. *Science* **330**: 192–196.
- Cayuela ML, Sanchez-Monedero MA, Roig A, Hanley K, Enders A, Lehmann J. (2013). Biochar and denitrification in soils: when, how much and why does biochar reduce  $N_2O$  emissions? *Sci Rep* **3**: 1732.
- Chan KY, Van Zwieten L, Meszaros I, Downie A, Joseph S. (2008). Using poultry litter biochars as soil amendments. *Aust J Soil Res* **46**: 437–444.
- Clayton H, McTaggart IP, Parker J, Swan L, Smith KA. (1997). Nitrous oxide emissions from fertilised grassland: A 2-year study of the effects of N fertiliser form and environmental conditions. *Biol Fert Soils* **25**: 252–260.
- Cuhel J, Simek M, Laughlin RJ, Bru D, Cheneby D, Watson CJ *et al.* (2010). Insights into the effect of soil pH on  $N_2O$  and  $N_2$  emissions and denitrifier community size and activity. *Appl Environ Microbiol* **76**: 1870–1878.
- Cusack DF, Silver W, McDowell WH. (2009). Biological nitrogen fixation in two tropical forests: Ecosystem-level patterns and effects of nitrogen fertilization. *Ecosystems* **12**: 1299–1315.
- Denman KL, Brasseur G, Chidthaisong A, Ciais P, Cox PM, Dickinson RE *et al.* (2007). Coupling between changes in the climate system and biogeochemistry. In: Solomon S, Qin D, Manning M, Marquis M, Averyt K, Tignor MMB *et al.* (eds) *Climate Change 2007: The physical science basis. Contribution of Working Group I to the Fourth Assessment Report of the Intergovernmental Panel on Climate Change*. Cambridge University Press: Cambridge, United Kingdom and New York, NY, USA, pp 499–587.
- Duce RA, LaRoche J, Altieri K, Arrigo KR, Baker AR, Capone DG *et al.* (2008). Impacts of atmospheric anthropogenic nitrogen on the open ocean. *Science* **320**: 893–897.
- Ducey TF, Ippolito JA, Cantrell KB, Novak JM, Lentz RD. (2013). Addition of activated switchgrass biochar to an arid subsoil increases microbial nitrogen cycling gene abundances. *Appl Soil Ecol* **65**: 65–72.
- Felber R, Hüppi R, Leifeld J, Neftel A. (2012). Nitrous oxide emission reduction in temperate biochar-amended soils. *Biogeosciences Discuss* **9**: 151–189.
- Flechar CR, Neftel A, Jocher M, Ammann C, Fuhrer J. (2005). Bi-directional soil/atmosphere  $N_2O$  exchange over two mown grassland systems with contrasting management practices. *Glob Change Biol* **11**: 2114–2127.
- Flessa H, Dorsch P, Beese F. (1995). Seasonal variation of  $N_2O$  and  $CH_4$  fluxes in differently managed arable soils in Southern Germany. *J Geophys Res-Atmos* **100**: 23115–23124.
- Flessa H, Wild U, Klemisch M, Pfaendner J. (1998). Nitrous oxide and methane fluxes from organic soils under agriculture. *Eur J Soil Sci* **49**: 327–335.
- Forster P, Ramaswamy V, Artaxo P, Berntsen T, Betts R, Fahey DW *et al.* (2007). Changes in atmospheric constituents and in radiative forcing. In: Solomon S, Qin D, Manning M, Marquis M, Averyt K, Tignor MMB *et al.* (eds) *Climate Change 2007: The physical science basis. Contribution of Working Group I to the Fourth Assessment Report of the Intergovernmental Panel on Climate Change*. Cambridge University Press: Cambridge, United Kingdom and New York, NY, USA, p 105.
- Galloway JN, Townsend AR, Erismann JW, Bekunda M, Cai ZC, Freney JR *et al.* (2008). Transformation of the nitrogen cycle: Recent trends, questions, and potential solutions. *Science* **320**: 889–892.
- Hsu S-F, Buckley DH. (2008). Evidence for the functional significance of diazotroph community structure in soil. *ISME J* **3**: 124–136.
- Jetten MSM. (2008). The microbial nitrogen cycle. *Environ Microbiol* **10**: 2903–2909.
- Jones CM, Graf DR, Bru D, Philippot L, Hallin S. (2013). The unaccounted yet abundant nitrous oxide-reducing microbial community: a potential nitrous oxide sink. *ISME J* **7**: 417–426.
- Jones CM, Stres B, Rosenquist M, Hallin S. (2008). Phylogenetic analysis of nitrite, nitric oxide, and nitrous oxide respiratory enzymes reveal a complex evolutionary history for denitrification. *Mol Biol Evol* **25**: 1955–1966.
- Joseph SD, Camps-Arbestain M, Lin Y, Munroe P, Chia CH, Hook J *et al.* (2010). An investigation into the reactions of biochar in soil. *Aust J Soil Res* **48**: 501–515.
- Jungkunst HF, Freibauer A, Neufeldt H, Bareth G. (2006). Nitrous oxide emissions from agricultural land use in Germany - a synthesis of available annual field data. *J Plant Nutr Soil Sc* **169**: 341–351.
- Keiluweit M, Nico PS, Johnson MG, Kleber M. (2010). Dynamic molecular structure of plant biomass-derived black carbon (biochar). *Environ Sci Technol* **44**: 1247–1253.
- Khodadad CLM, Zimmerman AR, Green SJ, Uthandi S, Foster JS. (2011). Taxa-specific changes in soil microbial community composition induced by pyrogenic carbon amendments. *Soil Biol Biochem* **43**: 385–392.
- Klappenbach JA, Saxman PR, Cole JR, Schmidt TM. (2001). rrndb: the ribosomal RNA operon copy number database. *Nucleic Acids Res* **29**: 181–184.
- Kumon Y, Sasaki Y, Kato I, Takaya N, Shoun H, Beppu T. (2002). Codenitrification and denitrification are dual metabolic pathways through which dinitrogen evolves from nitrate in *Streptomyces antibioticus*. *J Bacteriol* **184**: 2963–2968.
- Lam P, Kuypers MMM. (2011). Microbial nitrogen cycling processes in oxygen minimum zones. *Annu Rev Mar Sci* **3**: 317–345.
- Lehmann J, Joseph S. (2009). *Biochar for Environmental Management: Science and Technology*. Earthscan: London; Sterling, VA, USA.
- Loftfield N, Flessa H, Augustin J, Beese F. (1997). Automated gas chromatographic system for rapid analysis of the atmospheric trace gases methane,

- carbon dioxide, and nitrous oxide. *J Environ Qual* **26**: 560.
- Major J, Rondon M, Molina D, Riha SJ, Lehmann J. (2010). Maize yield and nutrition during 4 years after biochar application to a Colombian savanna oxisol. *Plant Soil* **333**: 117–128.
- Papen H, Vonberg R, Hinkel I, Thoene B, Rennenberg H. (1989). Heterotrophic nitrification by *Alcaligenes faecalis*—NO<sub>2</sub><sup>-</sup>, NO<sub>3</sub><sup>-</sup>, N<sub>2</sub>O, and NO production in exponentially growing cultures. *Appl Environ Microbiol* **55**: 2068–2072.
- Philippot L, Andert J, Jones CM, Bru D, Hallin S. (2011). Importance of denitrifiers lacking the genes encoding the nitrous oxide reductase for N<sub>2</sub>O emissions from soil. *Glob Change Biol* **17**: 1497–1504.
- Philippot L, Spor A, Henault C, Bru D, Bizouard F, Jones CM *et al.* (2013). Loss in microbial diversity affects nitrogen cycling in soil. *ISME J* **7**: 1609–1619.
- Ravishankara AR, Daniel JS, Portmann RW. (2009). Nitrous oxide (N<sub>2</sub>O): The dominant ozone-depleting substance emitted in the 21st century. *Science* **326**: 123–125.
- Reed SC, Cleveland CC, Townsend AR. (2007). Controls over leaf litter and soil nitrogen fixation in two lowland tropical rain forests. *Biotropica* **39**: 585–592.
- Reed SC, Cleveland CC, Townsend AR. (2011). Functional ecology of free-living nitrogen fixation: A contemporary perspective. In: Futuyma DJ, Shaffer HB, Simberloff D (eds) *Annual Review of Ecology, Evolution and Systematics*. Annual Reviews: Palo Alto, CA, USA, pp 489–512.
- Richardson D, Felgate H, Watmough N, Thomson A, Baggs E. (2009). Mitigating release of the potent greenhouse gas N<sub>2</sub>O from the nitrogen cycle—could enzymic regulation hold the key? *Trends Biotechnol* **27**: 388–397.
- Robertson GP. (2007). Nitrogen transformation. In: Paul EA (ed) *Soil Microbiology, Biochemistry and Ecology*. Springer: New York, NY, USA, pp 341–364.
- Rondon MA, Lehmann J, Ramirez J, Hurtado M. (2007). Biological nitrogen fixation by common beans (*Phaseolus vulgaris* L.) increases with bio-char additions. *Biol Fert Soils* **43**: 699–708.
- Ruser R, Flessa H, Schilling R, Steindl H, Beese F. (1998). Soil compaction and fertilization effects on nitrous oxide and methane fluxes in potato fields. *Soil Sci Soc Am J* **62**: 1587–1595.
- Ruser R, Flessa H, Russow R, Schmidt G, Buegger F, Munch JC. (2006). Emission of N<sub>2</sub>O, N<sub>2</sub> and CO<sub>2</sub> from soil fertilized with nitrate: Effect of compaction, soil moisture and rewetting. *Soil Biol Biochem* **38**: 263–274.
- Sanford RA, Wagner DD, Wu QZ, Chee-Sanford JC, Thomas SH, Cruz-Garcia C *et al.* (2012). Unexpected nondenitrifier nitrous oxide reductase gene diversity and abundance in soils. *P Natl Acad Sci USA* **109**: 19709–19714.
- Senga Y, Mochida K, Fukumori R, Okamoto N, Seike Y. (2006). N<sub>2</sub>O accumulation in estuarine and coastal sediments: The influence of H<sub>2</sub>S on dissimilatory nitrate reduction. *Estuar Coast Shelf S* **67**: 231–238.
- Singh B, Singh BP, Cowie AL. (2010a). Characterisation and evaluation of biochars for their application as a soil amendment. *Aust J Soil Res* **48**: 516–525.
- Singh BP, Hatton BJ, Singh B, Cowie AL, Kathuria A. (2010b). Influence of biochars on nitrous oxide emission and nitrogen leaching from two contrasting soils. *J Environ Qual* **39**: 1224–1235.
- Smith MS. (1982). Dissimilatory reduction of NO<sub>2</sub><sup>-</sup> to NH<sub>4</sub><sup>+</sup> and N<sub>2</sub>O by a soil *Citrobacter* sp. *Appl Environ Microbiol* **43**: 854–860.
- Smith MS. (1983). Nitrous oxide production by *Escherichia coli* is correlated with nitrate reductase activity. *Appl Environ Microbiol* **45**: 1545–1547.
- Smith MS, Zimmerman K. (1981). Nitrous oxide production by non-denitrifying soil nitrate reducers. *Soil Sci Soc Am J* **45**: 865–871.
- Smith P, Martino D, Cai Z, Gwary D, Janzen H, Kumar P *et al.* (2007). Agriculture. In: Metz B, Davidson OR, Bosch PR, Dave R, Meyer LA (eds) *In Climate Change 2007: Mitigation. Contribution of Working Group III to the Fourth Assessment Report of the Intergovernmental Panel on Climate Change*. Cambridge University Press: Cambridge, United Kingdom and New York, NY, USA.
- Sohi SP, Krull E, Lopez-Capel E, Bol R. (2010). A review of biochar and its use and function in soil. *Adv Agron* **105**: 47–82.
- Sorensen J, Tiedje JM, Firestone RB. (1980). Inhibition by sulfide of nitric and nitrous-oxide reduction by denitrifying *Pseudomonas fluorescens*. *Appl Environ Microbiol* **39**: 105–108.
- Steinbeiss S, Gleixner G, Antonietti M. (2009). Effect of biochar amendment on soil carbon balance and soil microbial activity. *Soil Biol Biochem* **41**: 1301–1310.
- Stevens RJ, Laughlin RJ, Malone JP. (1998). Measuring the mole fraction and source of nitrous oxide in the field. *Soil Biol Biochem* **30**: 541–543.
- Taghizadeh-Toosi A, Clough TJ, Condron LM, Sherlock RR, Anderson CR, Craigie RA. (2011). Biochar incorporation into pasture soil suppresses *in situ* nitrous oxide emissions from ruminant urine patches. *J Environ Qual* **40**: 468–476.
- Tanimoto T, Hatano K, Kim DH, Uchiyama H, Shoun H. (1992). Co-denitrification by the denitrifying system of the fungus *Fusarium oxysporum*. *FEMS Microbiol Lett* **93**: 177–180.
- Thomson AJ, Giannopoulos G, Pretty J, Baggs EM, Richardson DJ. (2012). Biological sources and sinks of nitrous oxide and strategies to mitigate emissions. *Philos T R Soc B* **367**: 1157–1168.
- Treusch AH, Leininger S, Kletzin A, Schuster SC, Klenk HP, Schleper C. (2005). Novel genes for nitrite reductase and *Amo*-related proteins indicate a role of uncultivated mesophilic Crenarchaeota in nitrogen cycling. *Environ Microbiol* **7**: 1985–1995.
- Uchimiya M, Wartelle LH, Lima IM, Klasson KT. (2010). Sorption of deisopropylatrazine on broiler litter biochars. *J Agr Food Chem* **58**: 12350–12356.
- van Zwieten L, Kimber S, Morris S, Downie A, Berger E, Rust J *et al.* (2010). Influence of biochars on flux of N<sub>2</sub>O and CO<sub>2</sub> from Ferrosol. *Aust J Soil Res* **48**: 555–568.
- Van Zwieten L, Singh B, Joseph S, Kimber S, Cowie A, Chan K. (2009). Biochar and emissions of Non-CO<sub>2</sub> greenhouse gases from soil. In: Lehmann J, Joseph S (eds) *Biochar for Environmental Management Science and Technology*. Earthscan: London, UK, pp 227–249.
- Vitousek PM, Cassman K, Cleveland C, Crews T, Field CB, Grimm NB *et al.* (2002). Towards an ecological understanding of biological nitrogen fixation. *Biogeochemistry* **57**: 1–45.
- Wallenstein MD, Myrold DD, Firestone M, Voytek M. (2006). Environmental controls on denitrifying communities and denitrification rates: Insights from molecular methods. *Ecol Appl* **16**: 2143–2152.

- Wang J, Zhang M, Xiong Z, Liu P, Pan G. (2011a). Effects of biochar addition on N<sub>2</sub>O and CO<sub>2</sub> emissions from two paddy soils. *Biol Fert Soils* **47**: 887–896.
- Wang JY, Pan XJ, Liu YL, Zhang XL, Xiong ZQ. (2012). Effects of biochar amendment in two soils on greenhouse gas emissions and crop production. *Plant Soil* **360**: 287–298.
- Wang S, Wang Y, Feng X, Zhai L, Zhu G. (2011b). Quantitative analyses of ammonia-oxidizing Archaea and Bacteria in the sediments of four nitrogen-rich wetlands in China. *Appl Microbiol Biotechnol* **90**: 779–787.
- Wrage N, van Groenigen JW, Oenema O, Baggs EM. (2005). A novel dual-isotope labelling method for distinguishing between soil sources of N<sub>2</sub>O. *Rapid Commun Mass Sp* **19**: 3298–3306.
- Yanai Y, Toyota K, Okazaki M. (2007). Effects of charcoal addition on N<sub>2</sub>O emissions from soil resulting from rewetting air-dried soil in short-term laboratory experiments. *Soil Sci Plant Nutr* **53**: 181–188.
- Yang WH, Weber KA, Silver WL. (2012). Nitrogen loss from soil through anaerobic ammonium oxidation coupled to iron reduction. *Nature Geosci* **5**: 538–541.
- Zhang AF, Bian RJ, Pan GX, Cui LQ, Hussain Q, Li LQ *et al*. (2012a). Effects of biochar amendment on soil quality, crop yield and greenhouse gas emission in a Chinese rice paddy: A field study of 2 consecutive rice growing cycles. *Field Crop Res* **127**: 153–160.
- Zhang AF, Liu YM, Pan GX, Hussain Q, Li LQ, Zheng JW *et al*. (2012b). Effect of biochar amendment on maize yield and greenhouse gas emissions from a soil organic carbon poor calcareous loamy soil from Central China Plain. *Plant Soil* **351**: 263–275.
- Zhao S, Fernald RD. (2005). Comprehensive algorithm for quantitative real-time polymerase chain reaction. *J Comput Biol* **12**: 1047–1064.
- Zheng JY, Stewart CE, Cotrufo MF. (2012). Biochar and nitrogen fertilizer alters soil nitrogen dynamics and greenhouse gas fluxes from two temperate soils. *J Environ Qual* **41**: 1361–1370.

Supplementary Information accompanies this paper on The ISME Journal website (<http://www.nature.com/ismej>)